SSRG International Journal of Civil Engineering
ISSN: 2348-8352/ https://doi.org/10.14445/23488352/IJCE-V13I6P110

Volume 13 Issue 6, 134-151, June 2026

Original Article

Level of Service Evaluation and Vehicle Emissions Using Microsimulations in SUMO, Huancayo, Peru

Zoraida Yazmin Meneses Marin[1], Alexandar Walter Riveros Bernardo[2], Jorge Elias Sanchez Capani[3], Christian Edinson Murga Tirado[4]

[1,2,3,4]*Department of Civil Engineering, Universidad Continental, Huancayo, Perú.*

[4]*Corresponding Author : cmurga @continental.edu.pe*

Received: 11 March 2026 Revised: 10 April 2026 Accepted: 09 May 2026 Published: 30 June 2026

Abstract *- Traditional traffic studies in Peru focus primarily on Level of Service (LOS) and control delay evaluation, frequently neglecting the environmental impact of vehicle emissions. In the present study, the relationship between intersection performance and vehicle emissions at signalized and unsignalized intersections is evaluated in Huancayo, Peru. Traffic simulations were carried out in SUMO and via the HBEFA4 emission model, for which 12 vehicle categories were implemented, in sharp contrast to previous studies. The assigned emissions class is based on exhaust aftertreatment technologies and historical Euro standards in Peru. The results reveal a disparity between the assigned LOS and control delay and the obtained emissions. The Southwestbound (SWB) approach achieved an optimal LOS A, yet it generated the highest emission mass of 41,078 g of CO2. In contrast, the minor street assigned as Lane Group 1–Y2 exhibited an LOS E but produced only 1,607.5 g of CO2 due to its low volume of 13 vehicles. The vehicle taxi category was identified as the primary emission source, followed by the category private car. It was concluded that traffic volume is a more dominant factor for CO2 emissions than control delay. Sustainable urban planning in Peru must integrate emission modeling and fleet modernization in conjunction with infrastructure-based delay reduction.*

Keywords *- Traffic Simulation, Emission Modelling, Vehicle Emission, Signalized Junction Analysis, Microsimulation Modeling.*

1. Introduction

According to the World Health Organization, nearly 90% of the world population lives in low air quality areas [1]. In this context, vehicle emissions: Carbon Dioxide (CO2), Nitrogen Oxides (NOx), and Particulate Matter (PM), are a key component of air quality degradation in urban areas.

Traffic engineering is key to reducing emissions through signal timing optimization or infrastructure improvement that maximizes vehicle flow, among other strategies [2]. However, a direct implementation to evaluate the impact of these strategies is neither practical nor cost-effective. In this regard, the use of computational techniques to quantify the impact of certain strategies prior to implementation on the traffic flow, fuel consumption, or emission reduction is useful [3].

Traffic simulation is generally classified into microscopic, mesoscopic, and macroscopic models. Microscopic models describe vehicle-to-vehicle interactions and include acceleration, deceleration, and lane changes [4]. Conversely, macroscopic models are based on aggregate variables: vehicle density and mean velocity [5]. Finally, mesoscopic approaches describe individual vehicles but not the vehicle-to-vehicle interaction [6].

Emission models can be classified as macroscopic or microscopic [7]. The former approach usually relies on average speeds, with COPERT serving as the reference model [8]. In contrast, the latter approach depends on velocity profiles that can be obtained via GPS-equipped vehicles, or through traffic simulators such as VISSIM, SUMO, or Matlab/Simulink, to name a few [9].

The German company PTV developed the microscopic simulation tool VISSIM, one of the most popular traffic flow simulation tools [10]. Under certain licensing, the VISSIM suite includes EnViVer Pro for emission calculations based on vehicle data. This module is built upon the microscopic emission and exhaust gas model VERSIT+, developed by the Netherlands Organization for Applied Scientific Research (TNO) [11]. The usual workflow includes using the velocity-time profiles derived from traffic flow simulations to obtain emission factors through VERSIT+ micro. Thereafter, the VISSIM-generated trajectories are imported into EnViVer, which uses VERSIT+ micro to calculate total emissions (g/h).

Quaassdorff et al. evaluated vehicle emissions at an urban roundabout in Madrid, Spain via the COPERT 4 macroscopic

approach and compared them to the VISSIM-EnViver microscopic approach [12]. Although both approaches showed correlation, the study concluded that the microscopic approach captures traffic congestion more accurately. In peak hours, the emission factors were 43% higher than in free-flow conditions, an effect that COPERT 4 underestimated. Similarly, Mesa-Vélez in Bogota, Colombia, used VISSIM and VERSIT+ to evaluate the impact of expanding public transit and infrastructure improvements on emissions reduction [13]. The effectiveness of these interventions was evaluated via the Level of Service (LOS) and Control Delay indicators.

Local studies in Peru are limited to LOS and Control delay assessments and exclude emissions evaluation. For instance, Díaz et al. [14] utilized VISSIM to analyze vehicle and pedestrian flow at a congested intersection in Jaén, Peru. The authors evaluated infrastructure improvements resulting in an LOS of B, which contrasted with the initial LOS of C. In the same way, Torres-Cortez et al. [15] in Huancayo, Perú, employed VISSIM to examine how infrastructure and signal timing improvements could enhance the LOS.

Simulation of Urban Mobility (SUMO) is a free and open-source microscopic simulation tool that is often used to study traffic flow. Baggio [16] carried out a comparison study of VISSIM and SUMO to simulate traffic flow and emissions calculation in Joinville, Brazil. The author concluded that the emission model PHEMlight, which is included in SUMO, and EnViver, based on VERSIT+, produce similar emissions results, and that vehicle fleet modernization and expanding public transit have the potential to reduce emissions by 55%.

Based on the conducted review, the majority of studies employ microsimulation approaches to study traffic flow and emissions. However, the restrictive commercial licensing of VISSIM and EnViver often restricts the replicability of such studies. In contrast, SUMO is an open-source platform and includes an HBEFA-based emission model by default, which enables full study replicability and transparency. Considering this, the current research conducts microsimulations using SUMO and its HBEFA4-based emission model, which has been the default since version 1.23.0. The novelty of this study lies in two key areas. First, most local traffic flow studies in Peru only evaluate LOS and control delay, ignoring emissions calculations. Second, a study that analyses signalized and unsignalized LOS and control delay and their impact on vehicle emissions is lacking. To the authors' knowledge, this is the first local study in Huancayo, Peru, to evaluate LOS and vehicle emissions simultaneously.

The research is conducted in Huancayo. First, the methodology is explained, including studied intersections, Lane Groups (LGs) definition, peak hour analysis, vehicle fleet characterization, and the application of Highway Capacity Manual (HCM) criteria used for LOS estimation. Finally, the results are presented, indicating the relation between control delay, LOS, and CO2 emissions for the defined LGs.

2. Materials and Methods

2.1. Road Network Geometry

Figure 1 shows the first study location, which consists of a signalized intersection and an unsignalized intersection. Geographically, it is located at coordinates -12.0494, -75.1956. In this location, the LGs are defined and are designated with the letter "X"; the following LGs are part of the signalized intersection: LG1-X1, LG2-X1, LG1-X2, LG1-X3, and LG2-X3. Meanwhile, the unsignalized LGs are LG2-X4 and LG1-X4. Figure 2 illustrates the defined LGs, as well as the street and avenue names for the first location.

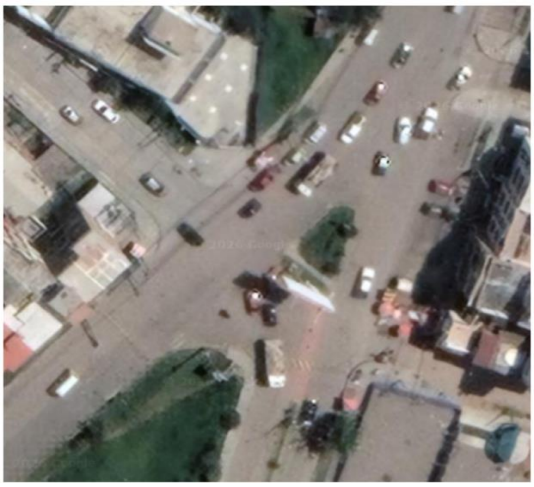

Fig. 1 Studied Intersection in the first location.

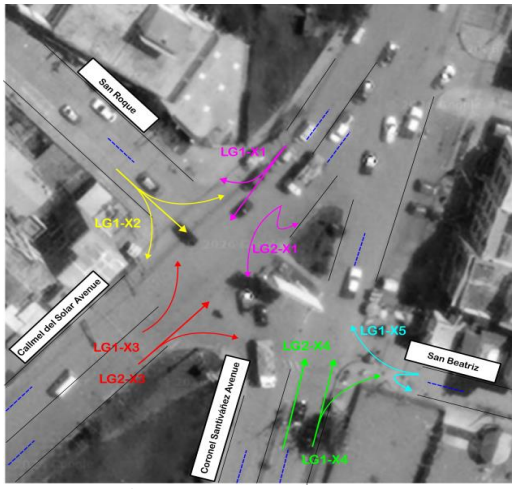

Fig. 2 Assigned LGs for the signalized and unsignalized intersection in the first location

Figure 3 depicts the second location, which features an unsignalized intersection and is located at coordinates -12.0460, -75.1946. Analogously, the LGs here are defined using the letter "Y" as shown in Figure 4. Table summarizes the LG information for the aforementioned locations.

Table 1. Lane Group definition for the studied intersections.

Lane Group (LG)	Direction	Street / Avenue
LG1-X1	Southwestbound (SWB)	Calmell del Solar Avenue
LG2-X1	Southwestbound (SWB)	Calmell del Solar Avenue
LG1-X2	Southeastbound (SEB)	San Roque Street
LG1-X3	Northeastbound (NEB)	Calmell del Solar Avenue
LG2-X3	Northeastbound (NEB)	Calmell del Solar Avenue
LG2-X4	Northeastbound (NEB)	Coronel Santiváñez Avenue
LG1-X4	Northeastbound (NEB)	Coronel Santiváñez Avenue
LG1-X5	Northeastbound (NEB)	San Beatriz Street
LG1-Y1	Southwestbound (SWB)	Calmell del Solar Avenue
LG2-Y1	Southwestbound (SWB)	Calmell del Solar Avenue
LG1-Y2	Eastbound (EB)	San Diego Street
LG1-Y3	Northeastbound (NEB)	Calmell del Solar Avenue
LG2-Y3	Northeastbound (NEB)	Calmell del Solar Avenue

In this study, SUMO 1.26 is used. The standard installation package includes OSMWebWizard and NETEDIT. The former permits the user to extract the base road infrastructure from OpenStreetMap (OSM), which is a free and editable worldwide map. The latter is SUMO's graphical network editor, and it was used to fix topological inaccuracies that often result from the imported OSM road infrastructure.

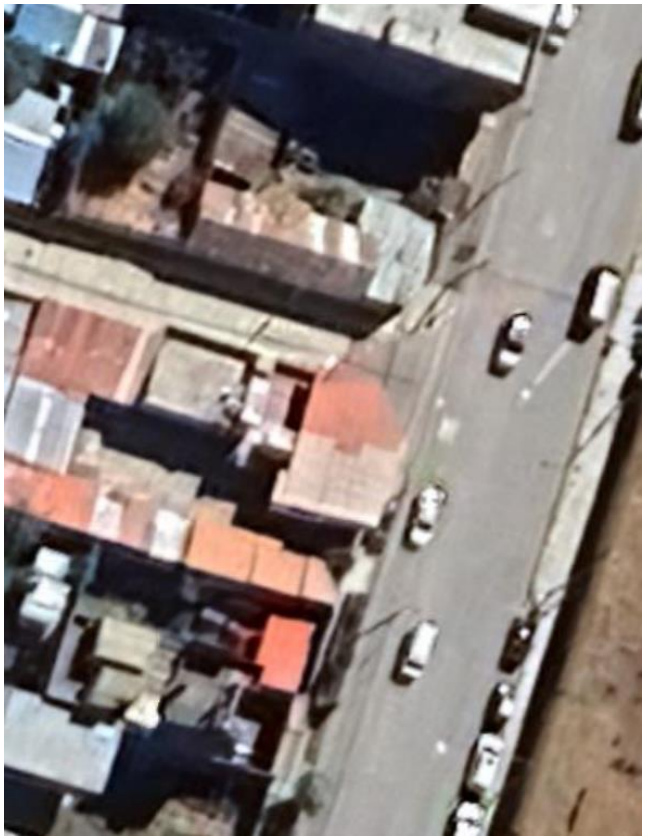

Fig. 3 Studied intersection in the second location

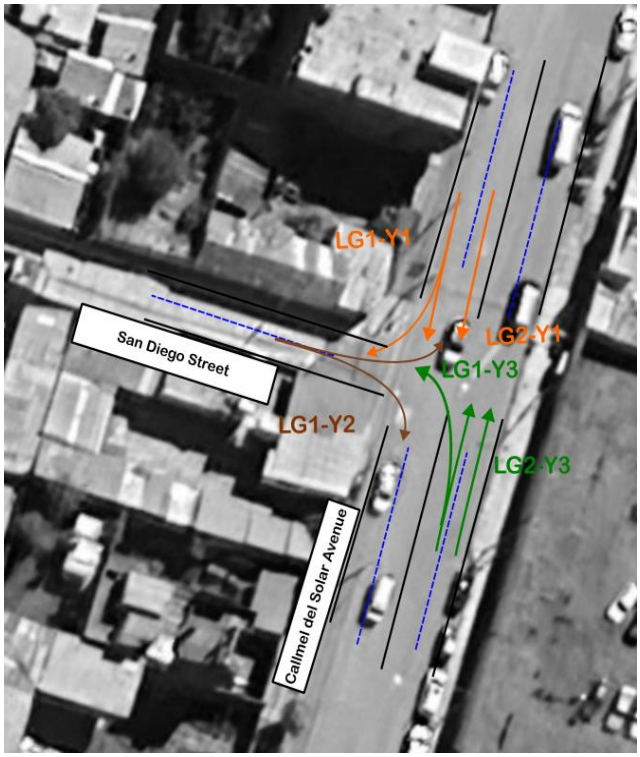

Fig. 4 Assigned LGs for the unsignalized intersection in the second location

Python 3.10 was utilized to run OSMWebWizard, as it was required to compute the bounding boxes of the selected two intersections.

In NETEDIT, edge properties such as the number of lanes, length, and width were modified to match the real conditions. In addition, the junction properties were edited to match the real conditions and to define LGs allowed movements of LGs. Each LG must have a defined "exit", which is defined as EX as shown in Figure 5.

The bi-directional road segment that corresponds to the Northeastbound is considered as a pair of edges in NETEDIT, where EX1 is represented by the id of -893125479#0 and the X3 edge is represented by 893125479#0. For this road segment, each edge consists of two lanes, and a width of 3.20 m was assigned to each lane. Considering the ID of each road segment and the designation of the LGs and EX edges, origin-destination paths are defined for the observed traffic demand in an .xml file. This described process was carried out for all road segments.

Figure 5 also depicts traffic light locations; their settings were configured in NETEDIT's traffic light mode to match the observed field conditions. Figure 6 depicts the traffic light phase inputs used according to these conditions. The total cycle length is 81s. For the first phase, which has a duration of 45s, the state string is GGGggGGgrrr. A capital letter G indicates priority to pass for vehicles, whereas a lower-case g indicates that vehicles must yield before passing. The letters y and r represent the yellow and red states, respectively.

The traffic lights settings and roadway geometry configurations are stored in a net.xml file. The origin-destination paths, vehicle types, and vehicle demand for each hour are set in an .xml route file. The specific vehicle types and demand distributions are described in the following section.

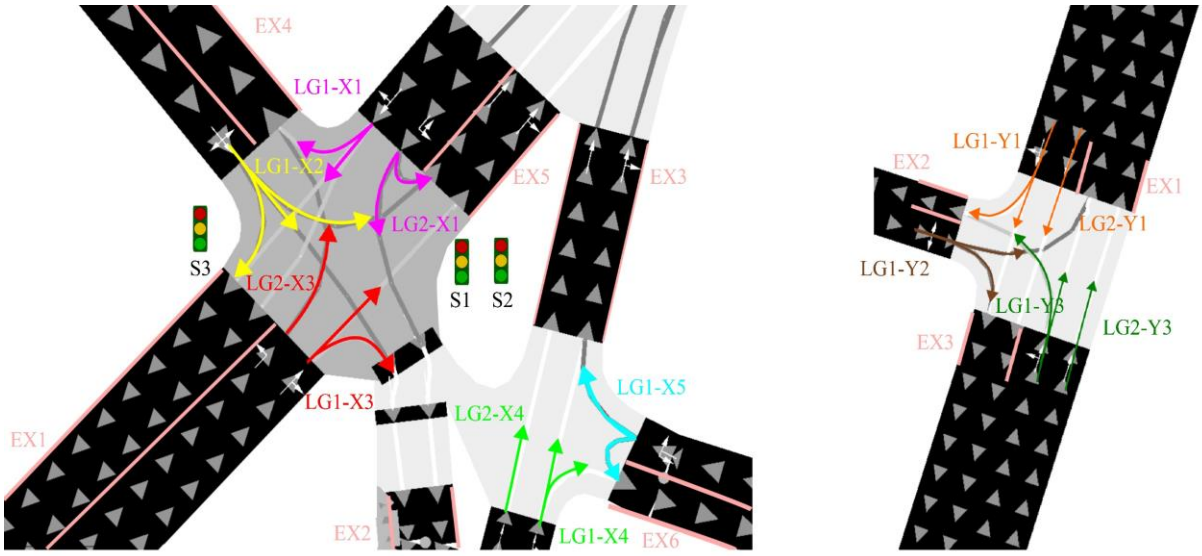

(a) **(b)**

Fig. 5 Road network configuration in NETEDIT for (a) Location 1 and (b) Location 2, illustrating the defined LGs, Exit Edges (EX), and traffic lights.

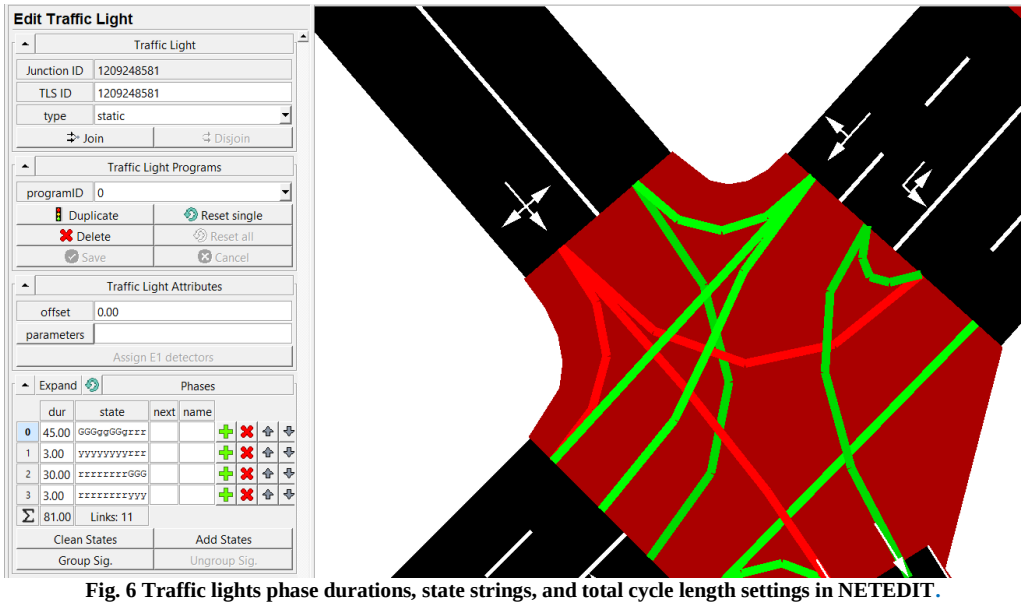

Fig. 6 Traffic lights phase durations, state strings, and total cycle length settings in NETEDIT.

2.2. Traffic Demand Analysis

The Turning Movement Count (TMC) is a method that consists of video recording and the categorization of vehicles by movements such as left-turn, right-turn, or through [17]. In the current study, the TMC method was used to obtain vehicle fleet demand and characterization.

For each of the defined locations, a 14-h recording from 8:00 AM to 10:00 PM is used. The data collection took place on a Monday for each of the locations, and the subsequent classification of vehicle movements in 15-minute intervals was done manually.

Figure 6(a) shows the traffic volume profile for Location 1, illustrating that the peak hour occurred between 5:45 AM and 6:45 PM. The peak hour volume reached 1,986 vehicles, and the maximum 15-minute volume is 522 vehicles, which corresponds to the time between 5:45 PM and 6:00 PM.

Figure 6(b) depicts the traffic volume profile for Location 2. In contrast to location 1, the peak hour occurred between 8:00 AM and 9:00 AM. The peak hour volume for this location was 1,854 vehicles, and the maximum 15-minute volume peaked at 541 vehicles between 8:15 AM and 8:30 AM.

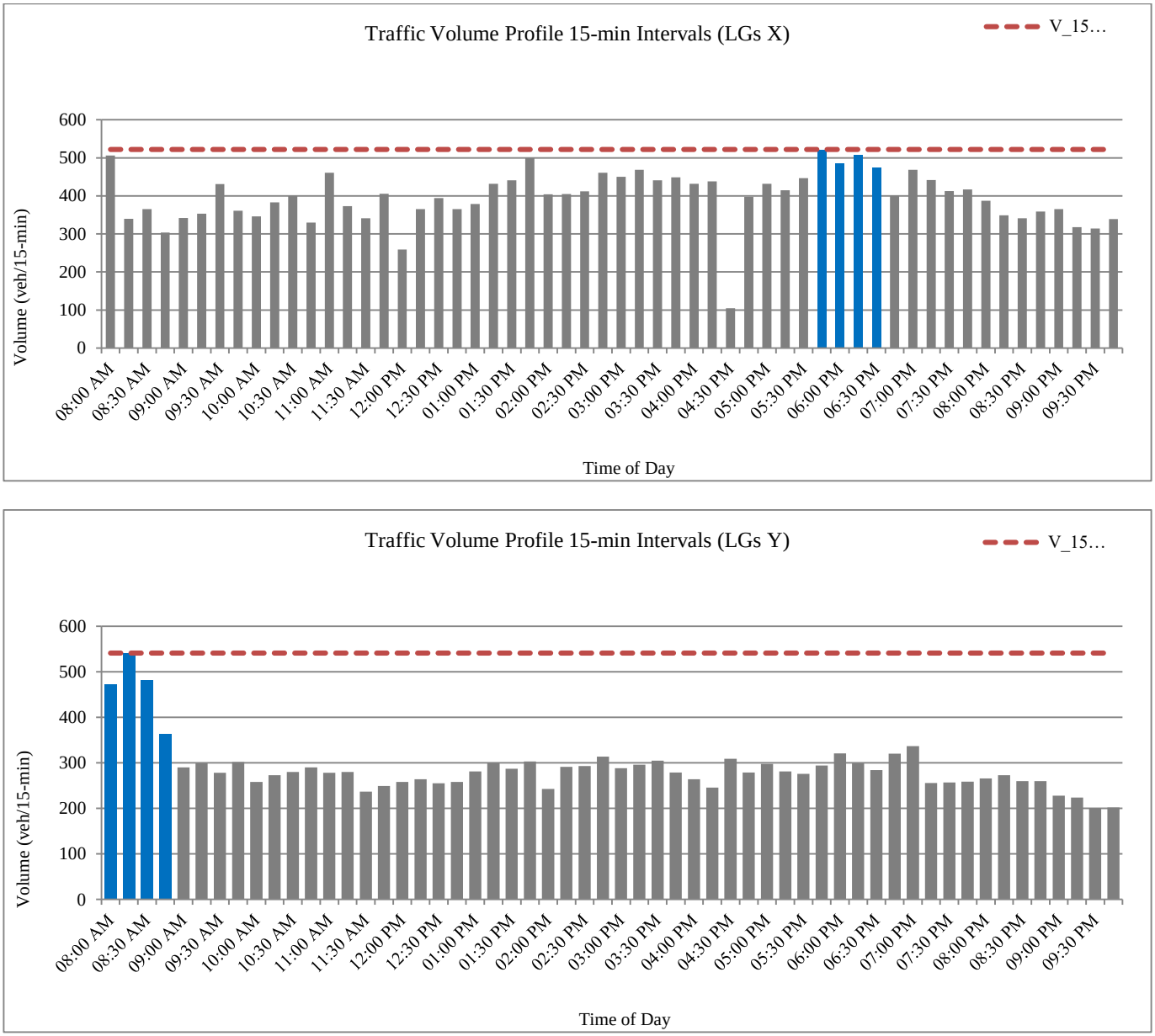

Fig. 7 Traffic volume at 15 min intervals from 8:00 AM to 9:45 PM for (a) LGs X and (b) LGs Y

Figure 7 shows the vehicle fleet characterization based on 12 observed vehicle categories. Figure 7(a) shows that at Location 1 during the peak hour, the most common vehicles are taxis, followed by private cars and shared taxis. The figure also shows the fleet composition for the entire 14-h observed data. Similarly, for Location 2, Figure 7(b) shows that at peak hour, the predominant vehicles are taxis, followed by shared taxis and combis. A combi is a type of Light Commercial Vehicle (LCV) frequently used for public transit; the term derives from the German word Kombinationskraftwagen.

2.3. Vehicle Fleet Characterization

2.3.1. HBEFA4-Based Emission Model in SUMO

SUMO's HBEFA4-based emission model estimates road-traffic emission using representative emission factors for many vehicle categories according to their fuel type and emission standard. The model uses the data from the Handbook Emission Factors for Road Transport (HBEFA) and fits it to a general continuous function for vehicle output rate, which estimates the emissions as a function of vehicle speed and acceleration [18]:

$$e(v,a) = c_0 + c_1 va + c_2 va^2 + c_3 v + c_4 v^2 + c_5 v^4$$

These coefficients vary depending on the pollutant and vehicle emission class.

2.3.2. Regulatory Context and Fleet Demographics

The assignment process of emission classes for each of the 12 observed vehicle categories is based on exhaust control technology and the historical active Euro emission standard in Peru. Starting in 2007, the new light-, medium-, and heavy-duty vehicles were required to meet Euro 3. The current Peru emission standard is Euro 4, which has been active since 2018 by means of the supreme decree No.025-2017-EM of the Ministry of Energy and Mines. The transition to Euro 6 is expected to be implemented in 2026.

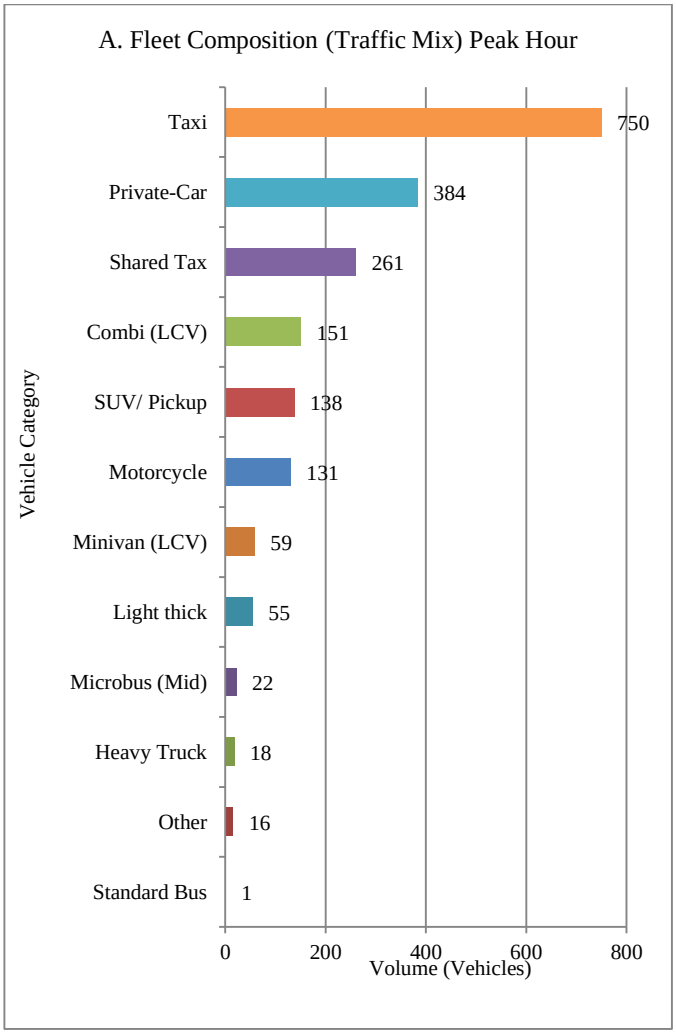

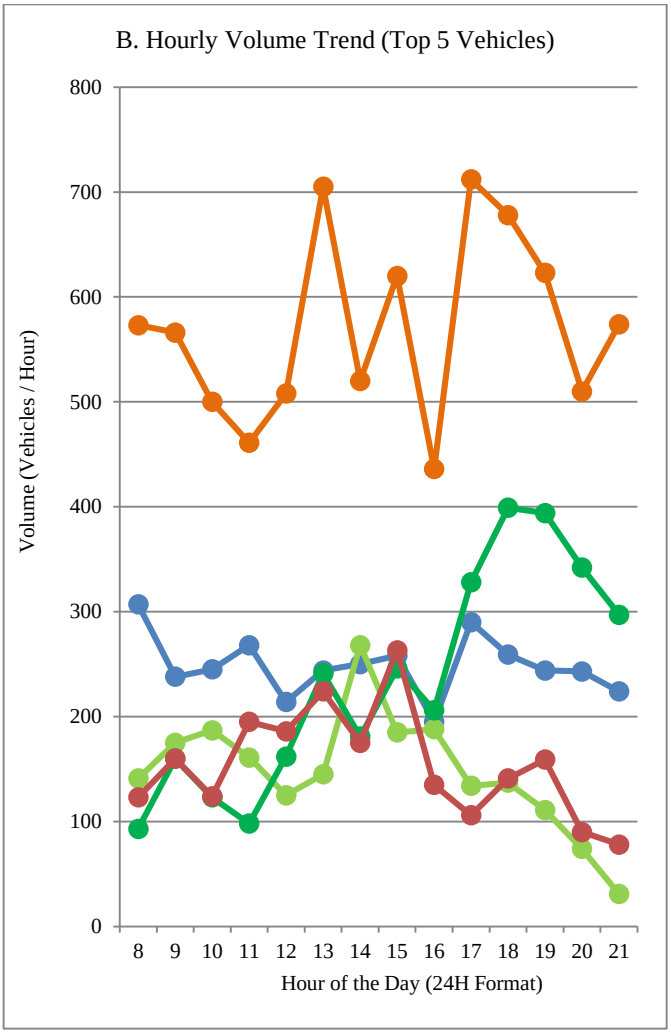

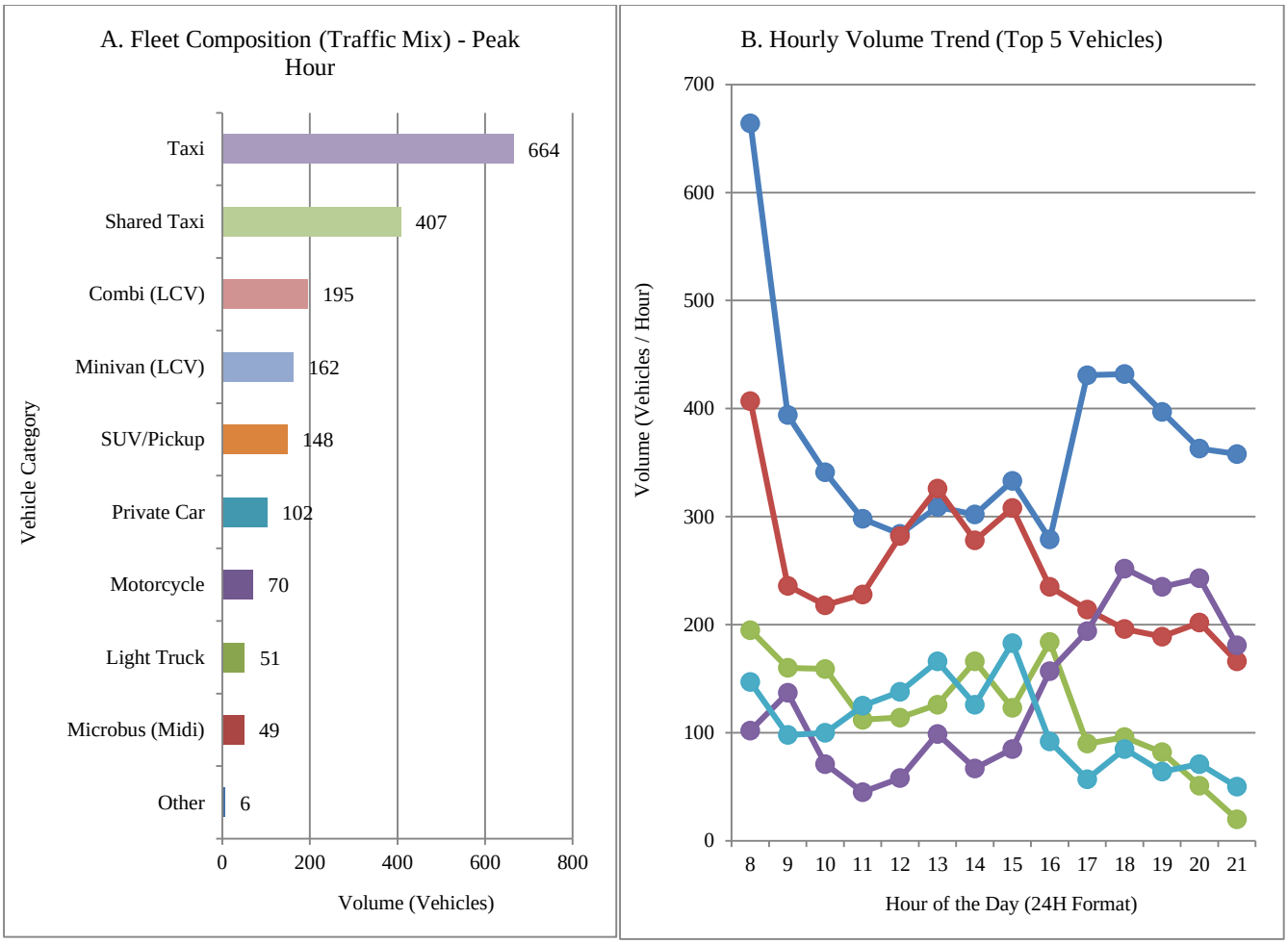

Fig. 1 Vehicle fleet composition at (a) Location 1 at the peak hour 5:45 PM - 6:45 PM and 14-h format and at (b) Location 2 at the peak hour 8:00 AM - 9:00 PM and 14-h format.

Although the observed vehicle fleet for the two locations offers detailed visual insight into the vehicle fleet longevity, a more rigorous classification can be deduced based on the exhaust control technology. To address the lack of data on the exhaust control technology for the observed 12 category vehicles, this study considered the detailed fuel and exhaust control technology characterization developed in Huancayo by Roman [19, 20].

The Ministry of Transport and Communications (MTC) of Peru reported that in 2024, the vehicle fleet in the Junín region reached 86,745, which is approximately 26% more than the 67,049 vehicles reported in 2016. It is worth mentioning that the MTC reports only include major vehicles; according to the MTC, this report excludes motorcycles and mototaxis [21]. Huancayo is one of the 9 provinces of Junín, and at the same time, Huancayo is divided into 28 districts. To collect the fuel and tech information in the Huancayo district, which shares its name with the province, Román considered a vehicle fleet of 61,504 that corresponded to the sum of the annually registered vehicles in Huancayo province, from 2002 to 2016, in the National Superintendency of Public Registries or SUNARP for its acronym in Spanish [20]. It should be noted that the fleet of 61,504 vehicles includes 24,547 motorcycles and mototaxis. Excluding these minor vehicles, the major vehicle fleet of Huancayo province is 36,957, representing 55% of the departmental total reported by the MTC. The proportion is consistent with the population and economic concentration in Huancayo province.

2.3.3. HBEFA Emissions Classes

Taking into account the vehicle fleet of Huancayo province as the study population, Román conducted a stratified probabilistic survey (n = 382) based on vehicular composition through video recording; 24,954 vehicles were observed. The aforementioned author developed a technological characterization of the vehicle fleet across seven categories [19]:

- Automobile and Station Wagon Category: Private vehicles / Taxi.
- Rural van
- Microbus Custer

- Sport Utility Vehicle (SUV)/pickup.
- Light Truck
- Motorcycle/Mototaxi
- Standard Bus

The process of assigning HBEFA emission classes to the observed 12 vehicle categories based on the Román fuel and technology [19] characterization and the historical active Euro emission standard in Peru is illustrated in Figure 8. Although the current national emission standard is Euro 4, the regional fleet has only increased by 26%. Therefore, the use of this historical vehicle exhaust control characterization remains a reasonable approximation. Figure 8 shows that Euro 3 is the newest emission class assigned.

Table 2 shows sample sizes from a stratified probabilistic survey based on in-situ video recording of the active fleet conducted by Román [19]. The table also shows the vehicle category, exhaust control technology, assigned emission class for HBEFA 4.0, and fuel type. For the "Automobile and Station Wagon Category", the fuel type follows the author's characterization that private vehicles operate mainly on gasoline, while taxi and shared-taxi services are predominantly converted to LPG dual-fuel systems. All the information considered until this point is defined within a SUMO route file (.rou.xml), which includes vehicle ID, type, route, time, lane, and speed. All these parameters are according to the assigned HBEFA emissions classification.

Table 2. Predominant fuel, exhaust control technology, and assigned emission class for the observed vehicle fleet.

Vehicle Category	Predominant Fuel	Exhaust Control Technology [19, 20]	HBEFA 4.0 Emission Class[a]	Survey Sample (*n*)
Private Car	Gasoline	100% 3-Way Catalyst / EGR	100% PC_petrol_Euro-3	280
Taxi / Shared Taxi	LPG / Dual (Gas)	100% 3-Way Catalyst / EGR	100% PC_LPG_petrol_Euro-3_(LPG)	
Combi / Minivan (LCV)	Diesel	49% EGR + Improved 51% None	49% LCV_diesel_N1-III_Euro-3 51% LCV_diesel_N1-III_Euro-1	43
SUV / Pickup	Diesel	70% EGR + Improved 30% None	70% LCV_diesel_N1-II_Euro-3 30% LCV_diesel_N1-II_Euro-1	13
Microbus custer	Diesel	70% EGR + Improved 30% Improved	70% UBus_Midi_le15t_Euro-II 30% UBus_Midi_le15t_Euro-I	13
Standard Bus	Diesel	50% EGR + Improved 50% None	50% UBus_Std_gt15-18t_Euro-II 50% UBus_Std_gt15-18t_Euro-I	3
Light Truck	Diesel	80% EGR + Improved 20% None	80% RT_le7.5t_Euro-III 20% RT_le7.5t_Euro-I	11
Heavy Truck	Diesel	80% EGR + Improved 20% None *(Extrapolated)*	80% RT_gt14-20t_Euro-III 20% RT_gt14-20t_Euro-I	N/A
Motorcycle / Mototaxi	Gasoline	100% None	100% MC_4S_le250cc_preEuro	19

[a] SUMO implementation requires the prefix HBEFA4/ before each class name (e.g., HBEFA4/PC_petrol_Euro-3).

[b] Heavy Truck (>14 t) was not independently surveyed by N. H. Román. Technology distribution extrapolated from the Light Truck (3–7.5 t) category, assuming comparable exhaust control adoption across diesel truck weight classes operating in Huancayo under Peru's uniform pre-2018 diesel emission standards.

The executable (.sumocfg) file uses the .net.xml file, which is the road network geometry, and the (.rou.xml), which is the vehicle fleet characterization according to the defined methodology in 2.2.1. As a result, a (tripinfo.xml) file that contains emissions for LGs and control delay is generated. Additionally, an (emissions_out.xml) file is generated, and it provides information to visualize the spatial distribution of CO2 emissions across the road network.

2.4. Level of Service Criteria

2.4.1. Signalized Intersections

According to the HCM 2010, the LOS can be characterized for the entire intersection or an approach using only Control delay values [22]. Control delays quantify the increase in travel time caused by traffic signals. The HCM also mentions that it is a surrogate measure of driver discomfort and fuel consumption.

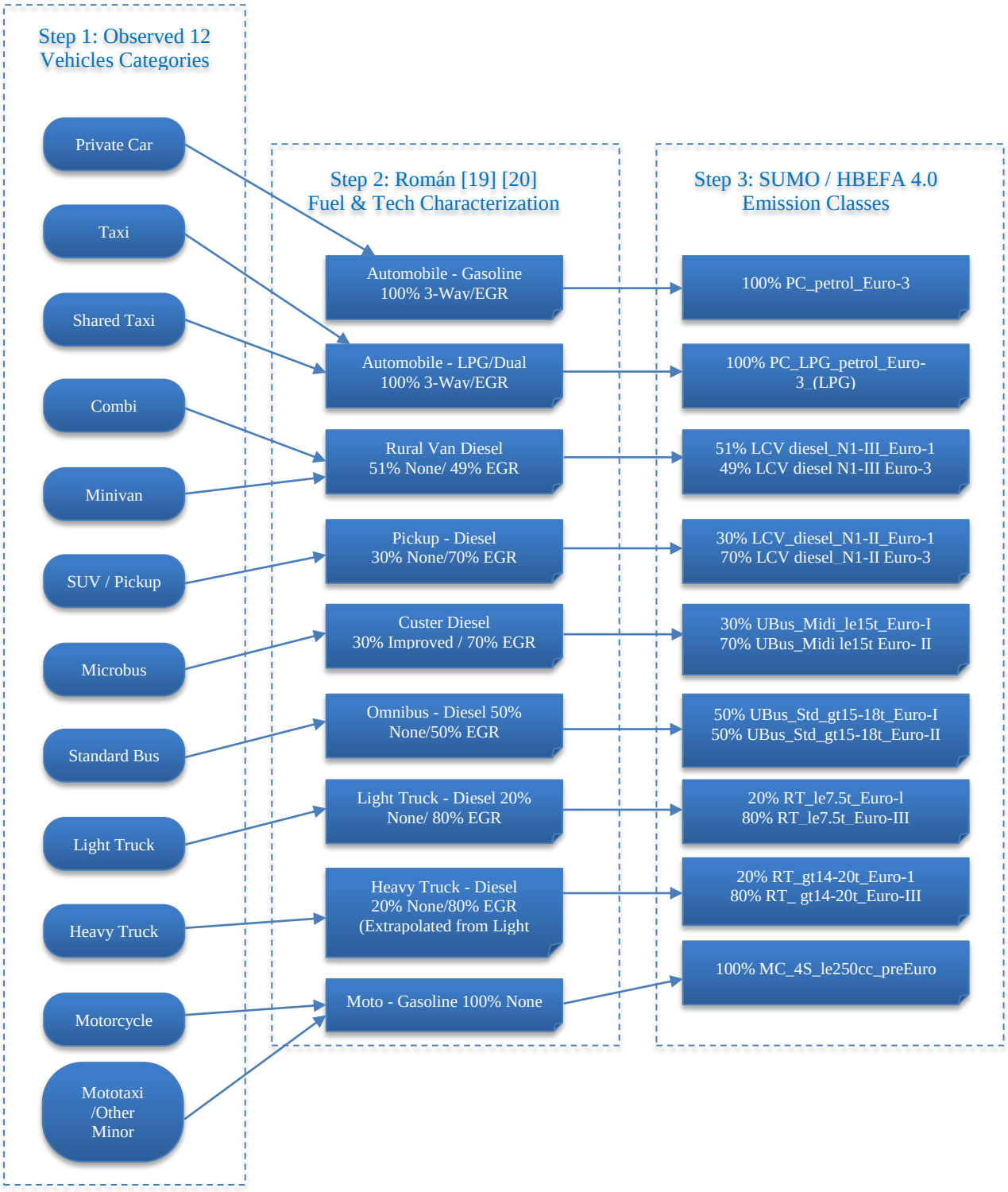

Fig. 2 Categorization process of the twelve observed vehicle types into HBEFA 4.0 Emission Classes.

In this study, LOS is defined solely by control delay. Since the present study reports LOS at the approach and intersection levels, not at the LG, the v/c > 1.0 override column does not apply to the reported results.

2.4.2. Unsignalized Intersections

The HCM 2010 states that for unsignalized intersections, the LOS is determined by the computed or measured control delay. LOS is not defined for major-street approaches for three reasons:

- Major streets through vehicles are assumed to experience zero delay.
- Due to the disproportionate number of vehicles on major streets, the resulting low average delays are not representative.
- A low average delay can mask LOS deficiencies for minor movements.

In the present study, major-street through movements such as LG1-X4, LG1-Y3, LG2-Y3, LG1-Y1, and LG2-Y1 are not assigned a LOS as they are assumed to experience no control delay due to the absence of stop control. Similarly, right-turn movements of LG1-X4 and left-turn movements from LG1-Y3 are assumed to operate with zero control delay for the same reason.

Table 3. LOS criteria for signalized intersection according to HCM 2010

Control Delay (s/veh)	LOS by Volume-to-Capacity Ratio[a]	
	v/c ≤ 1.0	v/c > 1.0
≤ 10	A	F
> 10–20	B	F
> 20–35	C	F
> 35–55	D	F
> 55–80	E	F
> 80	F	F
Note: For approach-based and intersection-wide assessments, LOS is defined solely by control delay.		

Table 4. LOS criteria for unsignalized intersection according to HCM2010

Control Delay (s/vehicle)	LOS by Volume-to-Capacity Ratio	
	v/c ≤ 1.0	v/c > 1.0
0–10	A	F
>10–15	B	F
>15–25	C	F
>25–35	D	F
>35–50	E	F
>50	F	F
Note: The LOS criteria apply to each lane on a given approach and to each approach on the minor street. LOS is not calculated for major-street approaches or for the intersection as a whole.		

It is important to clarify that HCM 2010 defines control delay as the total time loss due to negotiating an intersection, including deceleration and acceleration delay, queue move-up time, and stopped delay.

In SUMO, the tripinfo.xml file contains the timeLoss value defined as the cumulative time lost due to traveling below the desired speed, which inherently captures the components of control delay [23].

The FHWA traffic analysis toolbox (Volume III) emphasizes that the definition of delay differs from HCM, and that analysts must understand how delay is computed by the software used [24]. The timeloss value reported by SUMO is a conservative upper-bound estimated value of control delay, as it may include minor mid-block interactions not attributable to traffic control devices.

However, since the simulated signalized intersection presents short approaches, the major components of the time loss are attributed to traffic lights. Finally, a local study adopted the same procedure of deriving LOS from SUMO using timeloss [25].

2.5. Model Calibration

The GEH statistic is an empirical formula to compare the modeled vs actual counts. The following equation was used:

$$GEH = \sqrt{\frac{2(M-C)^2}{M+C}}$$

Where M represents the modeled volume, and C represents the real observed vehicles. A GEH value of less than 5 is considered a good fit. For the signalized intersection, a total of 1986 vehicles were observed at peak hour, while 2046 vehicles were simulated. The total difference is 60 vehicles and represents a 3%, which is acceptable. Table 5 disclosed the GEH value for each LG at Location 1 and showed that all LGs passed the GEH threshold. Figure 9 shows the GEH < 5 threshold and a bar chart of observed vs simulated vehicles.

Location 2 did not present any difference between the number of observed and simulated vehicles. This is attributed to the simpler road geometry and fewer edge configurations of Location 2, in contrast to Location 1.

Table 5. GEH Validation during the peak hour (17:45-18:45) by Lane Group

Lane Group	Observed	Simulated	GEH	Status
LG1-X1	318	318	0.00	PASS
LG2-X1	401	401	0.00	PASS
LG1-X2	175	235	4.19	PASS
LG1-X3	8	8	0.00	PASS
LG2-X3	300	300	0.00	PASS
LG1-X4	397	397	0.00	PASS
LG2-X4	376	376	0.00	PASS
LG1-X5	11	11	0.00	PASS

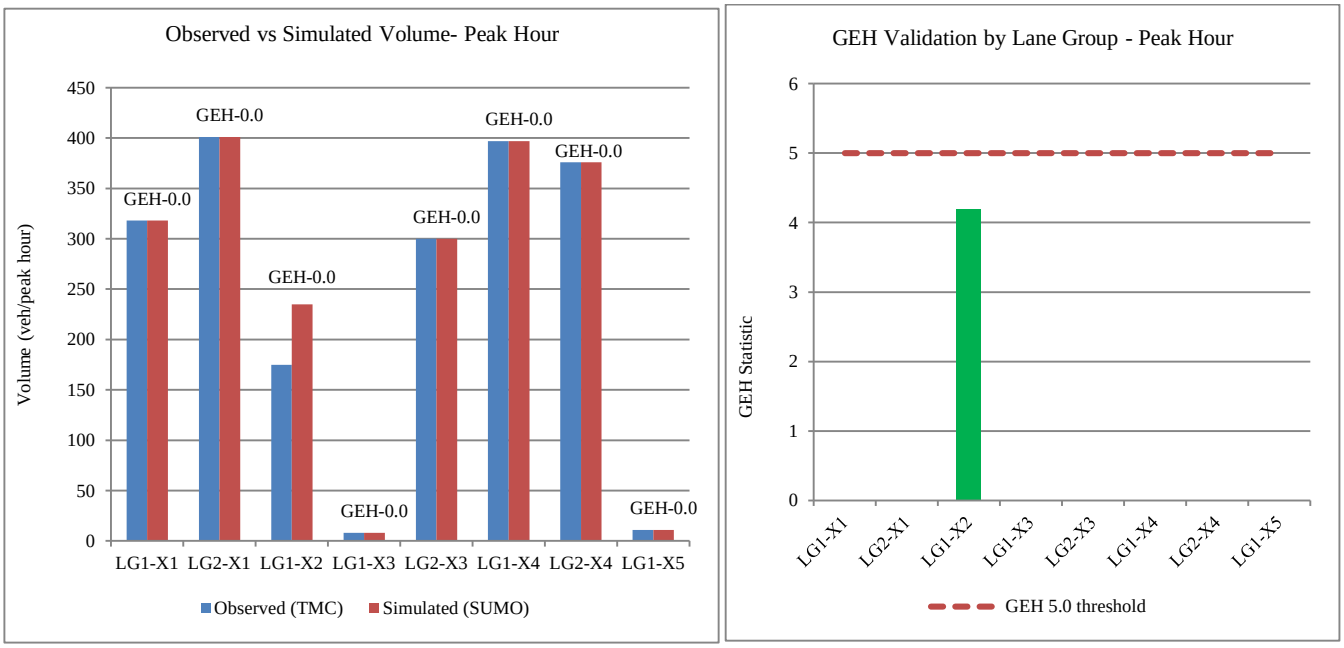

Fig. 10 GEH validation

3. Results

Figure 10(a) shows the average time loss for the unsignalized intersection at Location 1. As mentioned in the methodology section for unsignalized intersections, an LOS is assigned exclusively to the LG1-X5 right and LG1-X5 U-Turn, as they represent minor-street movements. In this case, LG1-X5 at peak hour only presents a volume of 11 vehicles. In stark contrast, LG1-X4 is considered a major street, as in peak hour, it exhibits 773 vehicles.

Figure 10(b) illustrates the resulting LOS assignment for the entire signalized intersection using the criteria of Section 2.3. The SWB approach, which consists of LG1-X1 and LG2-X1, exhibited an average time loss of 10 s, resulting in an assigned LOS A. For the SEB intersection, LG1X-2, the average delay was 31.7 s, corresponding to an LOS C. Finally, approaches NEB, LG1-X3, and LG2-X3 achieved LOS B.

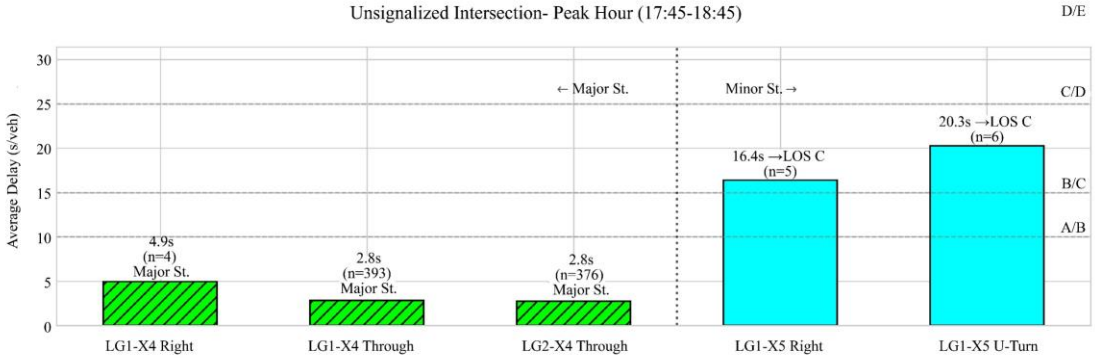

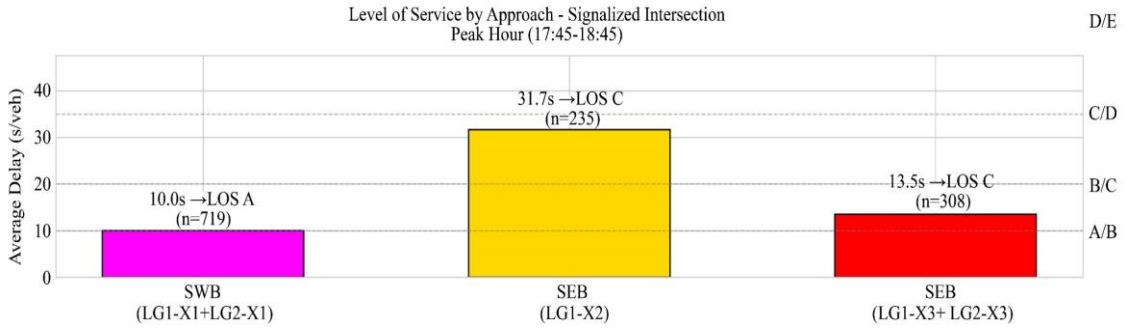

Fig. 3 Control delay results and LOS assignment for (a) signalized and (b) unsignalized intersection in Location 1. The major street movements represented by hatched bars are not assigned a LOS.

Figure 11 shows the average time loss results for the unsignalized intersection at Location 2. Similarly, an LOS of E is assigned to LG1-Y2 as it presents 13 vehicle volumes at peak hour. In stark contrast, LG1-Y3 presents 869 vehicles, and LG1-Y1 presents 972 vehicles; as a result, these LGs are major street thoroughfares.

The CO2 emissions at peak hour for the signalized intersection at Location 1 are illustrated in Figure 12. For the SWB approach that was assigned LOS A, 41,078 g of CO2 was obtained. Meanwhile, the NEB approach, LOS B, 20,997g of CO2 was evidenced. Finally, the SEB approach, categorized as LOS C, emitted 23,280g of CO2.

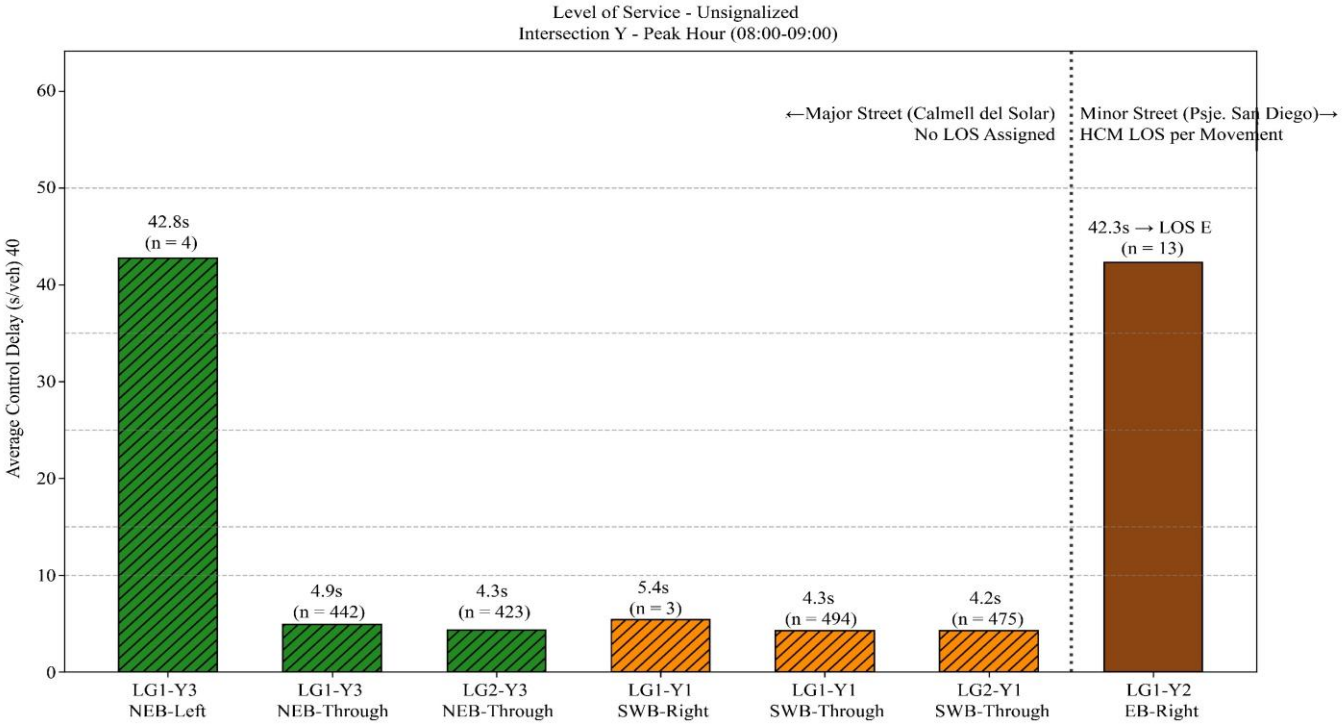

Fig. 4 Control delay results and LOS assignment at Location 2. The major street movements represented by hatched bars are not assigned a LOS.

Figure 13 displays the average time loss and CO2 emissions at location 1 by LGs. Within NEB, LG1-X3 presents an average delay of 51.7 s and 1,029g of CO2, representing the lowest CO2 result by LG at location 1. The LG2-X1 component of the SWB approach produced the highest CO2 emission value, 23,988g. Regarding the unsignalized intersection at Location 1, the LG1-X5 component evidenced the lowest CO2 value, 609 g. Meanwhile, the LG1-X4 component, corresponding to 14,241g of CO2, exhibited the highest value.

Regarding the CO2 vehicle emissions by LGs of the unsignalized intersection at Location 2. Figure 14 illustrates that LG1-Y2, which recorded an average timeloss of 42.3 s, emitted the lowest amount of CO2, 1,607.5g.

In contrast, LG1-Y1 exhibited a much lower average time loss of 4.3s; however, its total emissions reached 41,596 g, identifying it as the highest-emitting LG at Location 2.

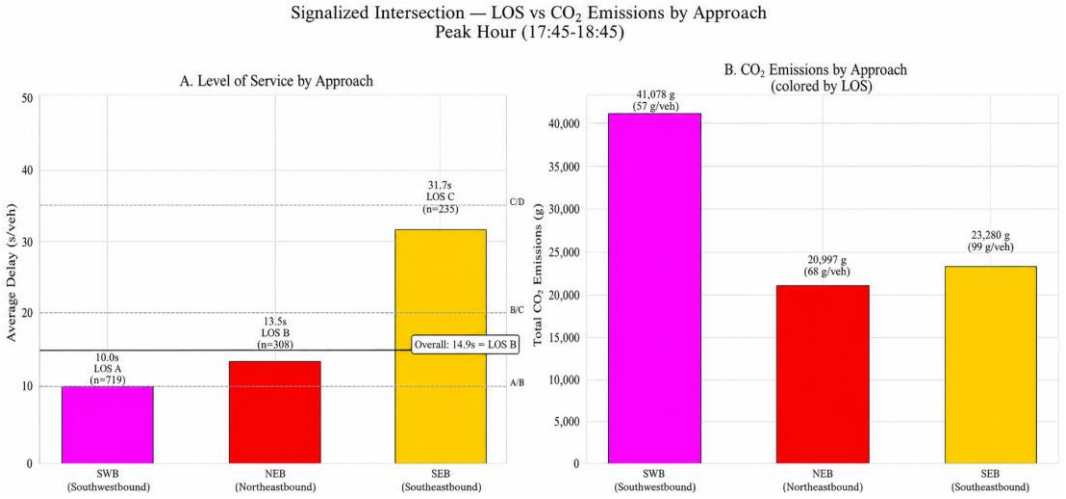

Fig. 5 Level of Service for the SWB, NEB, and SEB approach and their corresponding CO2 emissions at peak hour.

Figure 15 depicts a CO2 heatmap by LGs of the observed 12 vehicle categories at Location 1. Vehicle category taxi is the primary contributor of CO2 emissions at Location 1, and LG1-X2 presents the highest CO2 emissions associated with this vehicle class, 13,123 g. However, CO2 emissions associated with LG2-X1 and LG1-X1 that correspond to the SWB approach present a slightly higher emission value of 13,681 g. The private car category is the second contributor of emissions, as evidenced by 5,453 g of CO2 in LG1-X2. Regarding the unsignalized intersection at Location 1, LG1-X4 and LG2-X4 present higher CO2 concentrations for taxi and private car categories than LG1-X5, as a consequence of the low traffic volume of LG1-X5 at peak hour. In total, at Location 1, the vehicle category taxi at peak hour presents 40,741 g of CO2, while the private car presents 21,554.3 g.

Figure 16 illustrates the CO2 emission heatmap at the unsignalized intersection of Location 2. Similar to Location 1, the major-street LGs Y1 and Y3 present the highest CO2 emissions for the taxi, shared taxi, and Combi (LCV). The LG of Y1 in total presents 22,231 CO2 g, and the LG of Y3 presents 20,017 CO2 g. LG1-Y2 is a minor street, and low traffic volume causes low CO2 emissions for this LG. Some vehicle classes were not observed in this LG. However, LG1-Y2 presents an E LOS and the highest control delay at this location, but taxis only emitted 1,193 g. This fact highlights that in unsignalized urban environments, traffic volume is a more dominant factor in CO2 emissions than control delay. Overall, the LGs at Location 2 present higher emissions than those at Location 1 for the taxi and shared taxi categories. Furthermore, the low contribution from categories such as Mototaxis and Motorcycle remains consistent with the fleet composition observed during the peak hour; as well as the heatmap for Location 1, these do not represent a high emission class.

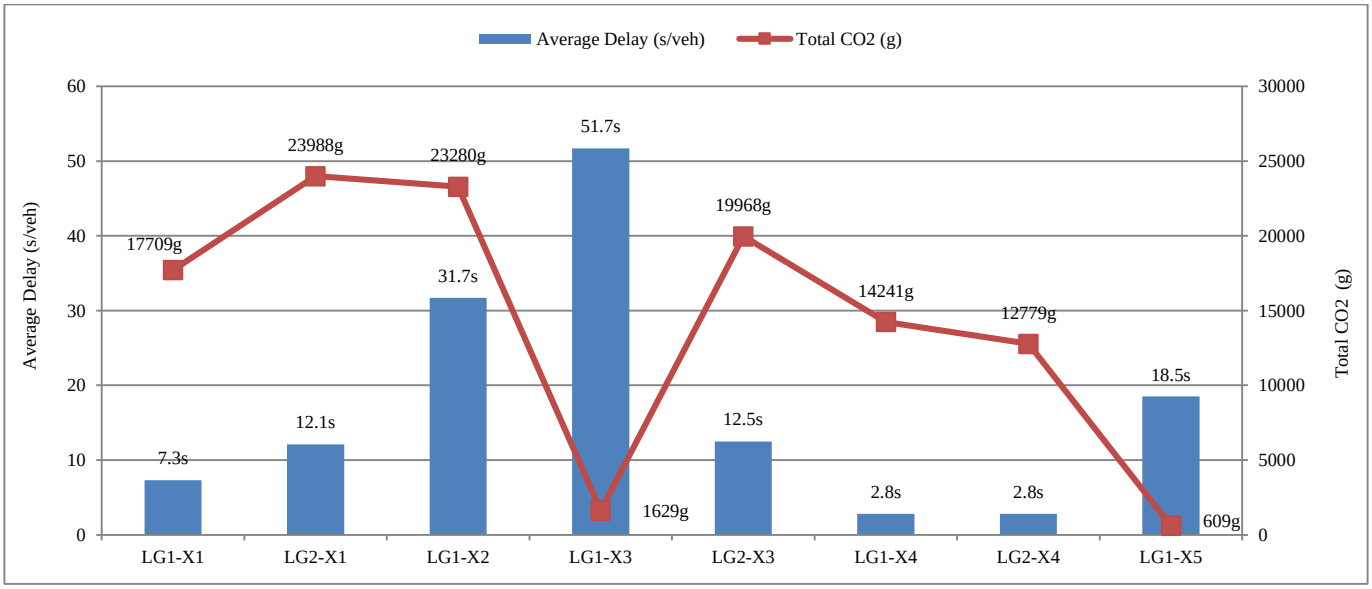

Fig. 14 Average delay and CO2 emissions by LGs at peak hour at Location 1.

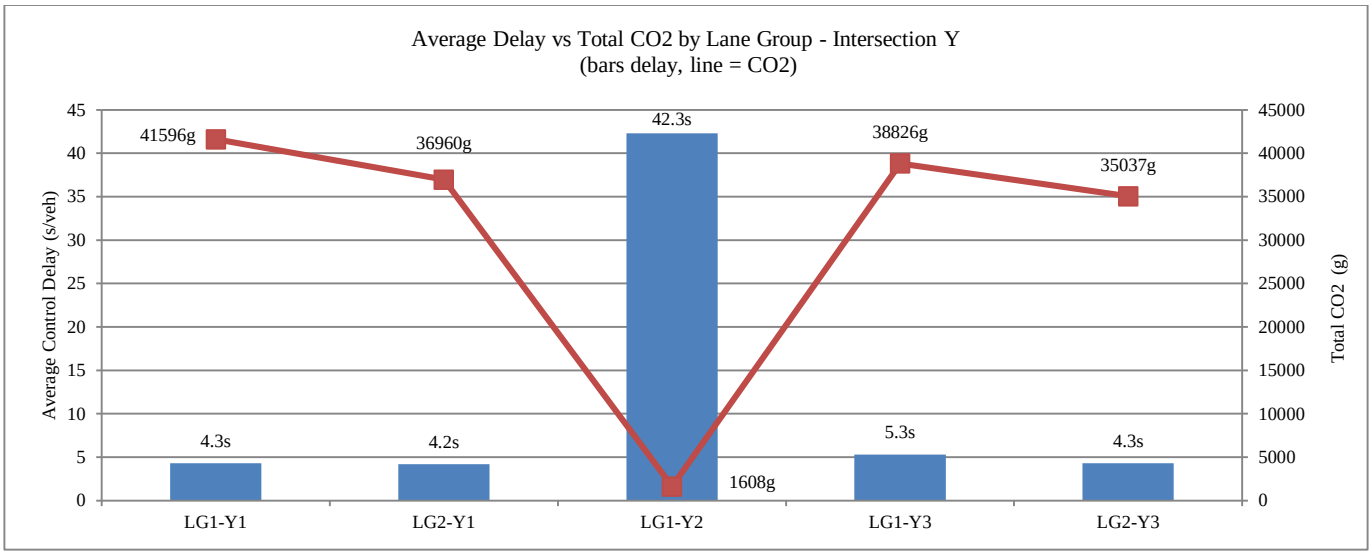

Fig. 15 Average delay and CO2 emissions by LGs at peak hour at Location 2.

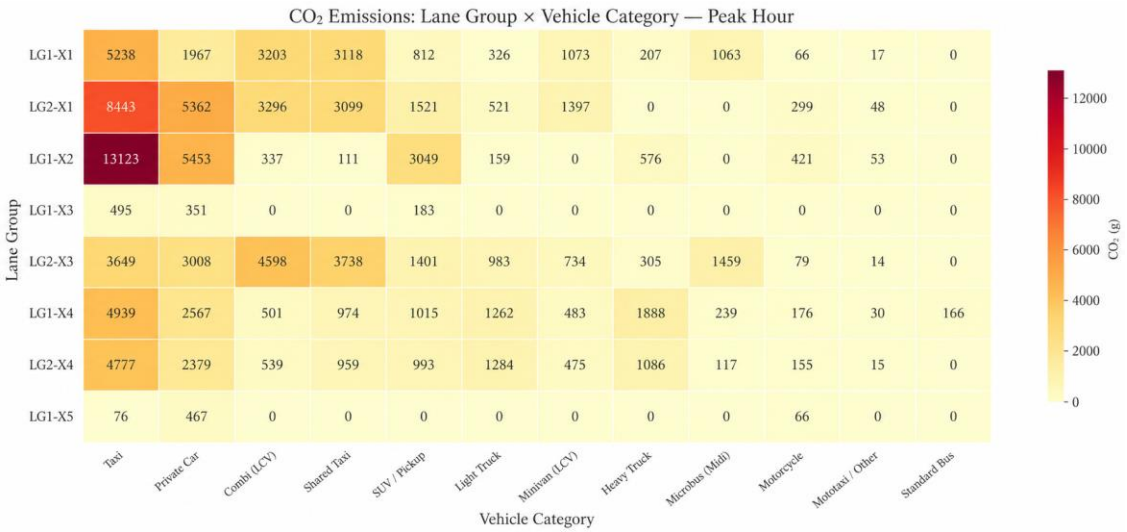

Fig. 16 Heatmap of CO2 emissions by LGs and vehicle category at peak hour 5:45 PM – 6:45 PM at Location 1.

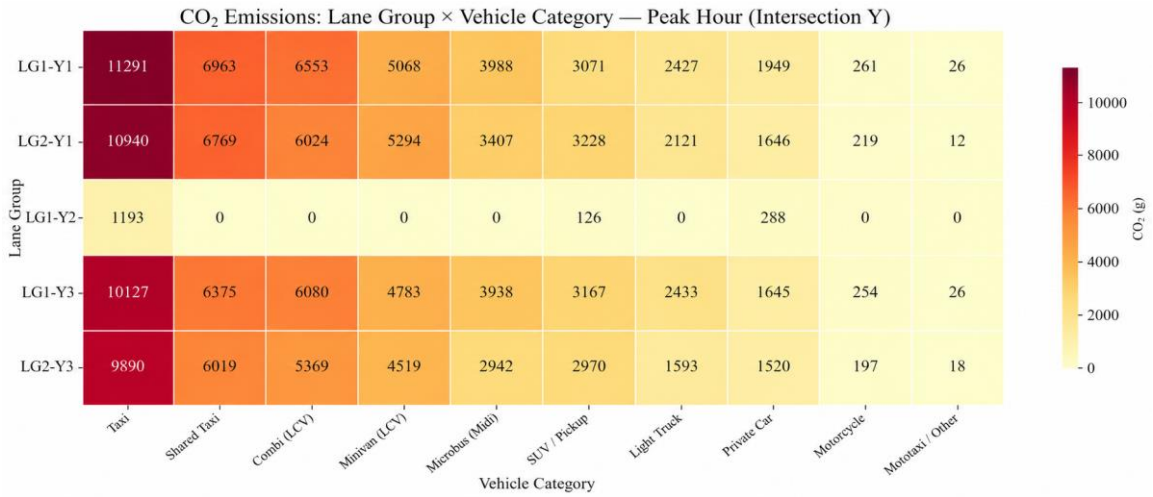

Fig. 17 Heatmap of CO_2 emissions by LGs and vehicle category at peak hour 8:00 AM – 9:00 AM at Location 2.

The spatial distribution of CO2 emissions during the peak hour is illustrated in Figure 17. Figure 17(a) confirms the identified LG hotspots. The SWB approach area, which comprises LG2-X1 and LG1-X1, clearly shows high CO2 spatial distribution indicated by the red hotspot. Regions that present yellow colors are associated with the LG1-X2, LG1-X4, and LG2-X4. The spatial distribution map shows that low traffic volume LG1-X5 does not represent a hotspot. Figure 17(b) shows that at Location 2, major-streets LGs of Y3 and Y1 present high CO2 concentration. In contrast, the low traffic volume of LG1-Y2 results in no CO2 concentration at peak hour, hence no hotspot is visible for this LG.

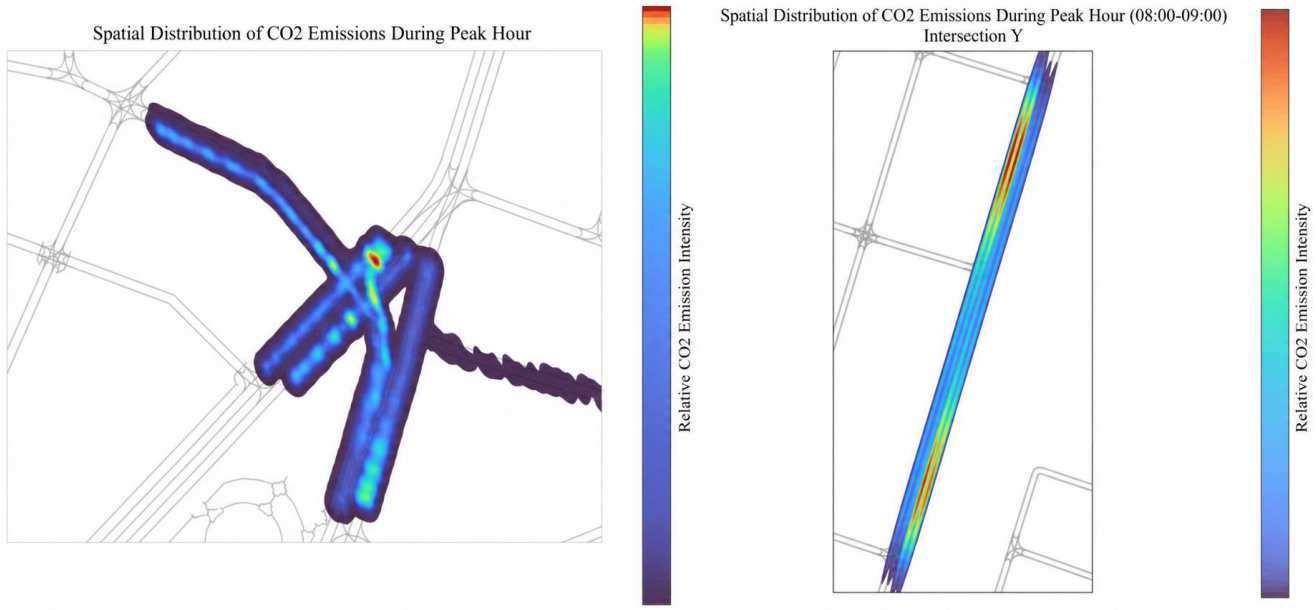

Fig. 18 Spatial distribution of CO_2 emissions during peak hours at the studied locations. (a) Location 1 (Signalized intersection context) and Location 2 (Intersection Y). The heatmaps represent the relative CO_2 emission intensity based on the spatial data generated by SUMO.

The Spatial distribution of CO2 for Location 1 and Location 2 is relevant as it represents the highest proportion among the pollutants analyzed during the peak hour, as shown in Table 5. At Location 1, the peak hour represents 7.4% of the total daily CO2 emissions, 1,526,902.2 g. Meanwhile, at the unsignalized intersection of Location 2, peak-hour CO2 emissions represent 11.8% of the total daily CO2 emissions, 1,326,011.2 g.

Table 6. Pollutant proportions at peak hour for the signalized intersection at Location 1 and the unsignalized intersection at Location 2

Intersection Type	PH	Vehicles	CO_2 (g)	CO (g)	HC (g)	NOx (g)	PMx (g)
Signalized / Unsignalized	17:45 - 18:45	2046	112,984.3	633.1	26.3	243.1	18.9
Unsignalized	08:00 - 09:00	1854	156,726.8	989.4	29.5	508.8	41.5

4. Discussion

Related studies were analyzed to contextualize the current research. A local study in Peru evaluated two signalized intersections and estimated CO, NOx, and VOCs using a single-vehicle equivalence for all the observed traffic [26]. However, the study does not estimate CO2 emissions, which, as was evidenced in the current study, presents the highest pollutant concentration and cannot be ignored.

In a signalized intersection in the city of Joinville, Brazil, and considering a baseline scenario where the vehicle fleet's average emissions standard is Euro 2, the author compared the use of ENVIVER VERSIT+ and PHEMLight. CO2 emissions, NOx, and PMx were calculated at peak hour in proportions of 279.34 kg, 1,004.67 g, and 115.51 g, respectively [16]. The author reported 2,089 vehicles at peak hour and made a vehicle fleet characterization on three categories: light-duty vehicles, buses, and heavy-duty vehicles. As an emission mitigation strategy, the author evaluated vehicle modernization in the Euro 5 standard. In Bogota, Colombia, LOS and emissions were calculated for a signalized corridor. Considering five types of vehicles in ENVIVER-VERSIT+, the pollutants CO2, NOx, and PM10 were estimated, revealing that CO2 represented the largest proportion. The author reported a LOS of C, D, and E that corresponds to 67% of movements [13]. A 30% transition to public transit caused 22 % less CO2 emissions, although some movements dropped to LOS E due to increased bus stop activity.

Beyond Latin American countries, other studies have evaluated vehicle emissions in congested areas. In Tashkent, Uzbekistan, 5,484 observed vehicles at peak hour were

reported [27]. Using ENVIVER-VERSIT+, the authors obtained CO2, NOx, and PMx, considering three types of vehicles. An overall LOS of C was assigned to the current roundabout infrastructure. In New Zealand [28], using four types of vehicles — motorcycle, bus, heavy-duty vehicle, and automobile under the Euro 4 standard, the author estimated CO2, CO, NOx, HC, and PMx. CO2 showed a higher proportion than other pollutants, followed by CO. The author found that increasing the use of electric vehicles to 20% has a higher potential to reduce emissions than carpooling and trackless trams. Table 6 summarizes the related studies discussed.

Table 7. Related studies comparison

Reference	Traffic Simulator	Emission Model	Observed Vehicles (Peak Hour)	Vehicle Categories	Emission Standard	Intersection Type	LOS	Calculated Pollutants
[26]	VISSIM	Not specified	2,568 / 2,283	Single vehicle equivalence	Not mentioned	Signalized	Not calculated	CO, NO_x, VOC
[27]	VISSIM	Not specified	5,484	3 Types (Auto, HDV, Bus)	Not mentioned	Signalized	Overall C	CO_2, NO_x, PM_x
[13]	VISSIM	ENVIVER-VERSIT+	Not mentioned	5 Types (HDV, Bus, Auto, etc.)	Not mentioned	Signalized	C, D, E	CO_2, NO_x, PM_{10}
[16]	SUMO	PHEMLight	2,089	3 Types (LDV, Bus, HDV)	EURO 2	Signalized	Not calculated	CO_2, NO_x, PM_x
	VISSIM	ENVIVER-VERSIT+						
[28]	SUMO	HBEFA 3.1	Not mentioned	4 Types (Moto, Bus, HDV, Auto)	EURO 4	Not mentioned	Not calculated	CO_2, CO, NO_x, HC, PM_x
This Study	SUMO	HBEFA 4	1,986 / 1,854	12 Types	EURO 1, 2, 3	Signalized / Unsignalized	A, B, C / E	CO_2, CO, NO_x, HC, PM_x

The presented methodology to estimate emissions based on exhaust control technology and historical Euro emission standards, combined with the assignment of HBEFA emission classes in SUMO, permits a robust characterization and modeling of vehicle emissions for the observed 12 vehicle categories. In addition, this research analyzed signalized and unsignalized intersections, which differ from previous studies. Furthermore, spatial distributions of CO2 were provided due to its significantly higher proportion compared to other pollutants.

The results of the present research evidenced high CO2 concentrations at the analyzed intersections, which is a primary cause of increasing greenhouse gas emissions. Conversely, pollutants such as PM, NOx, and CO are the most harmful to human health. In this context, emission mitigation strategies are discussed. The Euro 6 standard established a stricter emission limit for new vehicles, targeting lower NOx, HC, CO, and PM. However, to accomplish this, the used fuel must present low sulfur content. The virtually sulfur-free gasoline and diesel fuels (<10 ppm sulfur) are a fundamental prerequisite for the efficient operation of exhaust aftertreatment devices, named catalytic converters, Diesel, and Gasoline particulate filters [29]. Euro 6 was planned to be implemented in 2025 in Peru; however, supreme degree N.º 011-2025-EM was postponed to late 2026 due to local refineries' limitations in reaching the sulfur target levels [30]. In addition to efficient exhaust aftertreatment devices, local studies have proposed waste heat recovery technologies in vehicles as a potential approach to reduce emissions, although no direct implementations have been reported yet [31]. Regarding broader vehicle fleet modernization in Peru, a previous study found that adopting hybrid vehicles is the most suitable transition option based on charging infrastructure gaps, and cost accessibility, as hybrid vehicles are more affordable than electric vehicles, and not all type of hybrid vehicles requires charging stations [32]. The transition to Euro 6 and vehicle fleet modernization would modify the assigned emission classes in this study; their subsequent impact on intersection-level emissions could be evaluated as future scenarios using the proposed SUMO microsimulation methodology.

Main limitations of the conducted research include that the altitude factor of Huancayo, located at approximately 3,259 meters above sea level, was not considered in the emission calculations. It is well established that vehicles generate higher emissions at high altitudes due to lower air

density. In addition, while the assigned emissions classes were adapted to best match the observed vehicle types, they do not perfectly represent the local fleet, as the HBFA classes are based on European vehicle data. Future works should consider altitude correction factors for vehicle emissions at high altitudes and define localized vehicle categories, customizing both geometric parameters and emission rates to precisely reflect the reality of Peru.

5. Conclusion

This study evaluated the relationship between LOS, control delay, and vehicle emissions at signalized and unsignalized intersections in Huancayo, Peru, utilizing SUMO and the HBEFA4 emission model. The findings reveal a critical disparity between operational traffic efficiency and environmental impact. At the approach level, total traffic volume heavily outweighed control delay as the primary driver of CO2 mass emissions. For instance, the signalized SWB approach achieved an optimal LOS A, yet it generated the highest emission mass of 41,078 g of CO2 due to its substantial traffic volume of 719 vehicles. Similarly, at the unsignalized intersection, the major-street lane group LG1-Y1 exhibited a minimal delay of 4.3 s but emitted a peak of 41,596 g of CO2, driven by a heavy flow of 972 vehicles. In stark contrast, the minor-street LG1-Y2 suffered the highest delay of 42.3 s (LOS E) but produced the lowest total emissions,1,607.5 g, due to its exceptionally low volume of only 13 vehicles during the peak hour.

Furthermore, the disaggregated emission analysis by vehicle category identified taxis as the predominant environmental contributors across all studied lane groups. The granular data demonstrated that in approaches experiencing moderate congestion, such as LG1-X2, which presented 235 vehicles and LOS of C, taxis alone accounted for 13,123 g of CO2. These results underscore that relying solely on traditional LOS metrics is insufficient for sustainable urban planning.

References

[1] WHO Global Air Quality Guidelines, World Health Organization, 2021. [Online]. Available: https://www.who.int/publications/i/item/9789240034228

[2] Kapileswar Nellore, and Gerhard P. Hancke, "A Survey on Urban Traffic Management System Using Wireless Sensor Networks," *Sensors*, vol. 16, no. 2, pp. 1-25, 2016. [CrossRef] [Google Scholar] [Publisher Link]

[3] Mohammed Al-Turki et al., "On the Potential Impacts of Smart Traffic Control for Delay, Fuel Energy Consumption, and Emissions: An NSGA-II-Based Optimization Case Study from Dhahran, Saudi Arabia," *Sustainability*, vol. 12, no. 18, pp. 1-22, 2020. [CrossRef] [Google Scholar] [Publisher Link]

[4] Vladislav Krivda et al., "Use of Microsimulation Traffic Models as Means for Ensuring Public Transport Sustainability and Accessibility," *Sustainability*, vol. 13, no. 5, pp. 1-38, 2021. [CrossRef] [Google Scholar] [Publisher Link]

[5] H. K. Lee, H.W. Lee, and D. Kim, "Macroscopic Traffic Models from Microscopic Car-Following Models," *Physical Review E*, vol. 64, 2001. [CrossRef] [Google Scholar] [Publisher Link]

[6] Antonella Ferrara, Simona Sacone, and Silvia Siri, *Microscopic and Mesoscopic Traffic Models*, Freeway Traffic Modelling and Control, pp. 113-143, 2018. [CrossRef] [Google Scholar] [Publisher Link]

[7] Robin Smit, Leonidas Ntziachristos, and Paul Boulter, "Validation of Road Vehicle and Traffic Emission Models – A Review and Meta-Analysis," *Atmospheric Environment*, vol. 44, no. 25, pp. 2943-2953, 2010. [CrossRef] [Google Scholar] [Publisher Link]

[8] Feng Li et al., "Investigation and Prediction of Heavy-Duty Diesel Passenger Bus Emissions in Hainan Using a COPERT Model," *Atmosphere*, vol. 10, no. 3, pp. 1-14, 2019. [CrossRef] [Google Scholar] [Publisher Link]

[9] Maksymilian Mądziel, "Vehicle Emission Models and Traffic Simulators: A Review," *Energies*, vol. 16, no. 9, pp. 1-31, 2023. [CrossRef] [Google Scholar] [Publisher Link]

[10] Verena Zeidler et al., "Simulation of Autonomous Vehicles Based on Wiedemann's Car Following Model in PTV Vissim," *Proceedings of the 98th Annual Meeting of the Transportation Research Board (TRB)*, Washington, DC, USA, pp. 13-17, 2019. [Google Scholar] [Publisher Link]

[11] PTV Vissim 2022 User Manual, Karlsruhe: PTV Planung Transport Verkehr GmbH, PTV Group, 2022. [Online]. Available: www.ptvgroup.com

[12] Christina Quaassdorff et al., "Microscale Traffic Simulation and Emission Estimation in a Heavily Trafficked Roundabout in Madrid (Spain)," *Science of the Total Environment*, vol. 566-567, pp. 416-427, 2016. [CrossRef] [Google Scholar] [Publisher Link]

[13] Paula Natalia Mesa Vélez, "*Modeling of Environmental Emissions Associated with Mobility. Case Study: 13th Street Corridor between Boyacá Avenue and the Bogotá River Toll Plaza*," Colombian School of Engineering Julio Garavito, 2018. [Google Scholar] [Publisher Link]

[14] Salia Díaz, and Patricia Horna, "Analysis of Vehicular and Pedestrian Traffic at the Intersection of Francisco Orellana and Luna Pizarro using Simulations with the PTV Vissim Software in the City of Jaén," *Pakamuros Scientific Journal*, vol. 11, no. 3, pp. 43-56, 2023. [CrossRef] [Google Scholar] [Publisher Link]

[15] Torres Cortez et al., "*Diagnosis and Proposal to Reduce Queue Lengths in Public Transport at the Intersection of Av. Mariscal Castilla and Av. Evitamiento in the City of Huancayo, Using Traffic Microsimulation*," Peruvian University of Applied Sciences, pp. 1-88, 2020. [Google Scholar] [Publisher Link]

[16] Mariana Luersen Baggio, "*Comparison of Simulators SUMO and VISSIM for Measuring Traffic Flow Interactions and Vehicle Emissions: A Case Study in Joinville, Santa Catarina, Brazil*," Federal University of Santa Catarina, pp. 1-91, 2023. [Google Scholar] [Publisher Link]

[17] Harshit Maheshwari, Li Yang, and Richard W. Pazzi, "Traffic Intersection Simulation Using Turning Movement Count Data in SUMO: A Case Study of Toronto Intersections," *2025 21st International Conference on Distributed Computing in Smart Systems and the Internet of Things (DCOSS-IoT)*, Lucca, Italy, pp. 1-8, 2025. [CrossRef] [Google Scholar] [Publisher Link]

[18] Daniel Krajzewicz et al., "Second Generation of Pollutant Emission Models for SUMO," *Modeling Mobility with Open Data*, pp. 203-221, 2015. [CrossRef] [Google Scholar] [Publisher Link]

[19] Nilda Hilario Román, Hernán Baltazar Castañeda, and Walter Pardavé Livia, *Application of the International Vehicle Emissions (IVE) Model in Estimating Pollutant Emissions from Mobile Sources*, Development and Innovation in Engineering, pp. 8-13, 2020. [Google Scholar] [Publisher Link]

[20] Nilda Hilario Román, "*Pollutant Emissions from Vehicles in the Huancayo District*," Doctoral Thesis, National University of Central Peru, 2017. [Google Scholar] [Publisher Link]

[21] Statistics - Road Transport Services - Vehicle Fleet, Ministry of Transport and Communications, - Peruvian State Platform, MTC, 2025. [Online]. Available: https://www.gob.pe/institucion/mtc/informes-publicaciones/344892-estadistica-servicios-de-transporte-terrestre-por-carretera-parque-automotor

[22] Volume 3; 18-74 to 18-84: Highway Capacity Manual (HCM), 5th Edition, 2010. [Online]. Available: https://highways.dot.gov/safety/pedestrian-bicyclist/safety-tools/volume-318-74-18-84-highway-capacity-manual-hcm-5th

[23] Output - SUMO Documentation, 2026. [Online]. Available: https://sumo.dlr.de/docs/Simulation/Output/index.html

[24] Traffic Analysis Toolbox Volume III: Guidelines for Applying Traffic Microsimulation Modeling Software, 2019. [Online]. Available: https://ops.fhwa.dot.gov/trafficanalysistools/tat_vol3/sect6.htm

[25] J. M. Vilcas Painado, "*Traffic Control Mechanisms at the Service Level of Av. San Carlos, Section Jr. San Agustín and Jr. Santa Lucía, Huancayo-2024*," Thesis, Continental University, pp. 1-173, 2024. [Google Scholar]

[26] Ferrua Carrion Daniel, "*Influence of Vehicular Traffic on Air Pollution in the District of San Juan Bautista, Ayacucho Region, 2023*," Master Thesis, National University of San Cristóbal de Huamanga, pp. 1-134, 2023. [Google Scholar] [Publisher Link]

[27] Kudrat Kutlimuratov et al., "Modelling Traffic Flow Emissions at Signalized Intersection with PTV Vissim," *E3S Web of Conferences*, vol. 264, no. 1-12, 2021. [CrossRef] [Google Scholar] [Publisher Link]

[28] Jani Kaushalya, "*The Use of Microscopic Traffic Simulation Model for the Analysis of Vehicle Emission*," Master Thesis, pp. 1-121, 2025. [Google Scholar] [Publisher Link]

[29] Accelerating the Global Shift to a Cleaner On-Road Diesel Fleet, United Nations Environment Programme, 2025. [Online]. Available: https://www.unep.org/resources/policy-and-strategy/accelerating-global-shift-cleaner-road-diesel-fleet

[30] Supreme Decree No. 011-2025-EM - Regulations and legal documents - Ministry of the Environment - Peruvian State Platform, 2025. [Online]. Available: https://www.gob.pe/institucion/minam/normas-legales/6826108-011-2025-em

[31] Patrick Cuyubamba et al., "Design and Performance Study of the Heat Exchanger of a Fin-Based Thermoelectric Generator via Numerical Simulations," *2022 11th International Conference on Power Science and Engineering (ICPSE)*, Eskisehir, Turkey, pp. 34-39, 2022. [CrossRef] [Google Scholar] [Publisher Link]

[32] B. Rodríguez Pérez, and B. Rodríguez Pérez, "*Comparative Assessment of the Mass Introduction of Electric Vehicles in Peru*," *University and Society Journal*, vol. 13, no. 1, pp. 159-166, 2021. [Google Scholar] [Publisher Link]